Engineering a simple polarizable model for the molecular simulation of water applicable over wide ranges of state conditions

Ariel A. Chialvo and Peter T. Cummings

Citation: The Journal of Chemical Physics **105**, 8274 (1996); doi: 10.1063/1.472718
View online: http://dx.doi.org/10.1063/1.472718
View Table of Contents: http://scitation.aip.org/content/aip/journal/jcp/105/18?ver=pdfcov
Published by the AIP Publishing

Engineering a simple polarizable model for the molecular simulation of water applicable over wide ranges of state conditions

Ariel A. Chialvo and Peter T. Cummings
Department of Chemical Engineering, 419 Dougherty Engineering Bldg., University of Tennessee, Knoxville, Tennessee 37996-2200 and Chemical Technology Division, Oak Ridge National Laboratory, Oak Ridge, Tennessee 37831-6268

(Received 2 April 1996; accepted 5 August 1996)

We perform a systematic analysis of the relationship between the molecular geometry, the force-field parameters, the magnitude of the induced dipoles, and the resulting site–site microstructure of a model for water consisting of simple point charges plus a self-consistent point dipole polarizability. We constrain the model to represent the experimental values of the pressure and the configurational internal energy of water at ambient conditions, while keeping a permanent dipole moment of 1.85 D. The resulting force fields are then used to perform additional simulations at high temperature to determine the effect of polarizabilities on the site–site structure, and to make contact with neutron scattering experiments as well as *ab initio* simulation results. We show that the parameterization of the model is possible for $0 \leqslant R_{OM} \leqslant 0.25$ Å, where R_{OM} is the oxygen-to-negative charge distance along the bisectrix of the H–O–H angle, resulting in total dipole moments from 2.88 to 3.03 D, with polarization energies accounting for 40%–57% of the total configuration internal energy of water. These results, in conjunction with the behavior of the short range site–site correlation functions, highlight the shortcomings of the simple point charge approximation for the polarization behavior at short intermolecular distances, and give a meaningful reference from which we can attempt to overcome these defects. © *1996 American Institute of Physics.*
[S0021-9606(96)51242-0]

I. INTRODUCTION

Simple molecular force fields for water are usually described by an arrangement of point charges located in a well defined molecular geometry.[1] Because these charges cannot vary in response to the changing local electric field, these models are unable to account for the considerable polarization effects ever present in condensed polar fluids. Yet, for simulation purposes, the many-body polarization contributions are typically described in an *average* way by pairwise additive interactions of enhanced dipole moments (over the corresponding gas phase values) which are obtained by fitting the Coulombic charges of a model to the fluid thermodynamic properties of the real system. This assumption, that the potential energy can be expressed as a sum over pair interactions, is the most frequently used even though it has been recognized that many-body polarization effects account for a substantial contribution to the properties of the condensed phase of highly polar fluids such as water,[2] especially on the dielectric constant.[3]

While the pairwise assumption might work well to treat many-body interactions as effective two-body interactions in fluids showing quasi-isotropic polarization effects[3]—such as in pure water where the charge distribution can be considered centered at the oxygen—this approximation fails for systems in which the isotropic polarization breaks down—such as in the neighborhood of an ion in solution—i.e., when the direction of the average dipole moment does not coincide with the bisector of the H–O–H bond angle.

Another important defect of these nonpolarizable water models hinges upon the fact that they cannot describe the two-body interactions of an isolated molecular pair, i.e., the behavior at low density, and concomitantly, the many-body interactions of the condensed phase as effective pairwise potentials, without running into undesired strong state dependent force-field parameters.[4,5] Thus nonpolarizable water models suffer from the lack of transferability, and therefore, they cannot describe accurately the phase behavior at conditions other than the one used in the parameterization. Note that an alternative state dependence parameterization for pure water, which in principle could have helped in this matter, does not appear to be as successful as we might have expected.[5] Despite this common shortcoming, simple pair potential models such as the SPC,[6] SPC/E,[7] TIP4P,[8] and ST2[9] have been quite successful in reproducing most thermophysical properties of water at ambient conditions, and in some cases, they have been able to describe qualitatively well the entire phase envelope,[10,11] including the properties at supercritical conditions.[12]

As improvements on these simple pair potential models, numerous polarizable water models have recently been developed to cope with the shortcomings of the simple models.[13–24] While these models show improvement in the description of some water properties, their overall performance is quite disappointing in comparison to that of their nonpolarizable counterparts, if we consider that the polarizable model captures the physical picture of water molecule more accurately than the nonpolarizable one. In fact, most polarizable models have not been able to describe simultaneously the thermodynamics, the structure, and consequently, the dielectric behavior of real water. Furthermore, in that context, it appears unclear whether this failure is either

the result of the inadequacy of the models, their parameterization, or both. Note that among the few exhibiting reasonable agreement with experimental data at ambient conditions, i.e., microstructural, thermodynamic, and dielectric properties,[18,24] the agreement is usually obtained at the expense of having a permanent dipole moment considerably larger than the gas-phase value of 1.85 D. Possible exceptions to the above comment are the recently developed TIP4P-FQ model,[21] the *ab initio* based NCC model,[25] and the TIP4P-like model of Brodholt *et al.*[22] if we are willing to accept that the first and second models predict a negative pressure (-160 ± 30 and -1180 ± 470 atm, respectively) for ambient water, and that the third model overpredicts the dielectric constant by a factor of 2.

The primary goal of this work is the development of a transferable model capable of reproducing the pressure, the configurational internal energy, and the site–site pair correlation functions at 298 K and 1.0 g/cc (conditions at which we have the most reliable experimental data) while maintaining a permanent dipole moment of 1.85 D. By transferable we mean that the resulting model should be able to account properly for the two-body interactions at gaslike densities, and the many-body interactions at liquidlike densities, without invoking state-dependent force-field parameters. In pursuing this goal we first seek answers to the following (superficially) simple questions: Is it possible to determine the non-Coulombic force fields (e.g., the Lennard-Jones' size and energy parameters) such that the resulting polarizable model reproduces, within simulation accuracy, the thermodynamic properties of water at ambient conditions? If so, what other requirements must the model fulfil to give a reasonable description of the system's structure?

Answers to these questions are a necessary step in gaining some valuable insight toward the development of a successful polarizable water model for the molecular simulation of aqueous solutions over a wide range of state conditions, i.e., from ambient to supercritical. In order to answer these questions we need to perform a systematic analysis of the dependencies between the molecular geometry (e.g., the H–O–H angle and the distances O–H and O–M, where M is the site of the negative charges located along the H–O–H bisector toward the H sites) and the force-field parameters, the magnitude of the induced dipoles, and the resulting site–site microstructure, by constraining the system to satisfy the experimental values of the pressure and the configurational internal energy of water at ambient conditions. Because the SPC geometry has already been studied,[15,18,26] we decided to analyze first the effect of the O–M distance on the polarization behavior, and consequently, on the effective quadrupole moment of an otherwise SPC model (i.e., $R_{OM}=0$). Furthermore, to determine the polarization behavior at near-critical and supercritical conditions, and to test an earlier claim regarding the polarization behavior of water,[12] we use the model to simulate a high temperature system, for which experimental structural data are available from neutron scattering.[27]

The paper is organized as follows. In Sec. II we describe the model, its parameterization, and the simulation methodology. In Sec. III we present the simulation results for the model's thermodynamics, force fields, and structure at ambient and high temperature conditions for a series of geometries. Finally, we close with a discussion and highlight of relevant conclusions.

TABLE I. Electrostatic parameters of the water models as a function of the adopted geometry.

R_{OM} (Å)	q_O (e^-)[a]	Q_{xx}[b]	Q_{yy}[b]	Q_{zz}[b]
0.0	−0.669 6	1.61	−1.61	~0.0
0.05	−0.733 07	1.76	−1.75	−0.008
0.10	−0.809 83	1.96	−1.92	−0.04
0.15	−0.904 08	2.22	−2.12	−0.10
0.20	−1.024 45	2.56	−2.36	−0.19
0.25	−1.180 92	3.01	−2.66	−0.35
	Experimental[c]	2.63	−2.50	−0.13

[a]Permanent charge corresponding to a dipole of 1.85 D.
[b]Quadrupole moments in D Å units.
[c]Reference 46.

II. MODEL DESCRIPTION AND PARAMETERIZATION

A. Simple point charges plus a self-consistent point dipole polarizability

The starting point of our analysis is the rigid geometry of the SPC water model,[6] i.e., a planar configuration with an H–O–H angle of 109.5° and an O–H bond length of 1.0 Å. The electrostatic charges are initially located on the three SPC sites, with magnitudes such that the permanent dipole moment is that of the isolated water molecule, i.e., 1.85 D.[28] Subsequently, we analyze the situation for which the negative charges are located along the H–O–H bisector, a distance R_{OM} toward the H sites (see Table I and Fig. 1). While some readers might argue that the SPC geometry is incompatible with the gas phase water geometry, in that neither its H–O–H angle nor its O–H bond length agrees with those of the water dimer,[28] our objective here is not to mimic the gas phase water geometry but rather to obtain a plausible intermolecular potential model able to describe properly the two-body dipolar interactions. An initial overconstraining in the model parameterization, e.g., by enforcing simultaneously the gas phase geometry, dipole, and quadrupole moments might complicate unnecessarily the model's parameterization

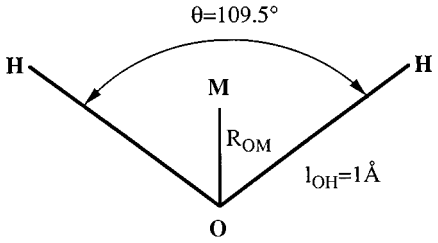

FIG. 1. Schematic representation of the water model geometry.

and could obscure the relationships between specific force-field parameters, and the resulting microstructure and polarization behavior.

With this geometry, the model consists of a Lennard-Jones O–O pair plus the M–M and M–H electrostatic pair interactions. In addition, we include an isotropic-linear point dipole polarizability at the center of mass (or at the O site) to account for the many-body polarizability effects. For a system of N water molecules, with s (3 or 4) permanent charges and a point dipole polarizability, the induced dipole moment on the center of mass of molecule i is given by

$$\begin{aligned}\mathbf{p}_i &= \alpha \mathbf{E}_i \\ &= \alpha(\mathbf{E}_i^q + \mathbf{E}_i^p).\end{aligned} \tag{1}$$

In Eq. (1) α is the scalar molecular polarizability, $\mathbf{E}_i$ is the total electric field on the center of mass of molecule i, whose contribution from the permanent charges of sites γ on molecule j is given by

$$\mathbf{E}_i^q = \sum_{j \neq i,}^{N} \sum_{\gamma=1}^{s} q_j^\gamma \frac{\mathbf{r}_{i,j\gamma}}{|\mathbf{r}_i - \mathbf{r}_{j\gamma}|^3} \tag{2}$$

while the corresponding polarization contribution at the center of mass of molecule i is given by

$$\mathbf{E}_i^p = \sum_{j \neq i}^{N} \mathbf{T}_{ij} \cdot \mathbf{p}_j . \tag{3}$$

In the preceding equations we used the following notation: $\mathbf{r}_{i\beta,j\gamma} = \mathbf{r}_{i\beta} - \mathbf{r}_{j\gamma}$, where $\mathbf{r}_{i\gamma} = \mathbf{r}_i + \mathbf{r}_i^\gamma$ and $\mathbf{r}_i$ are the vector positions of site γ and center of mass of molecule i, respectively. In Eq. (3) $\mathbf{T}_{ij}$ is the symmetric dipole tensor,

$$\mathbf{T}_{ij} = \frac{1}{r_{ij}^3} \left(\frac{3\mathbf{r}_{ij}\mathbf{r}_{ij}}{r_{ij}^2} - \mathbf{I} \right) \tag{4}$$

and $\mathbf{I}$ is the unit tensor.

The total electrostatic energy for this system is given by[29]

$$\begin{aligned}U &= U_{qq} + U_{\mathrm{pol}} \\ &= U_{qq} + U_{qp} + U_{pp} + U_{\mathrm{self}}\end{aligned} \tag{5}$$

with the charge–charge contribution U_{qq}

$$U_{qq} = 0.5 \sum_{j \neq i}^{N} \sum_{\beta,\gamma}^{s} \frac{q_i^\beta q_j^\gamma}{|\mathbf{r}_{i\beta} - \mathbf{r}_{j\gamma}|}; \tag{6}$$

the charge–dipole contribution U_{qp}

$$U_{qp} = -\sum_{i=1}^{N} \mathbf{p}_i \cdot \mathbf{E}_i^q ; \tag{7}$$

the dipole–dipole contribution U_{pp}

$$U_{pp} = -0.5 \sum_{j \neq i}^{N} \mathbf{p}_i \cdot \mathbf{T}_{ij} \cdot \mathbf{p}_j , \tag{8}$$

and the self-polarizability term U_{self},

$$U_{\mathrm{self}} = \left(\frac{0.5}{\alpha} \right) \sum_{i=1}^{N} \mathbf{p}_i^2 . \tag{9}$$

Now, from Eqs. (6)–(9) and recalling Eq. (1) we have that

$$\begin{aligned}U_{\mathrm{pol}} &= -\sum_{i=1}^{N} (\mathbf{p}_i \cdot \mathbf{E}_i^q - 0.5\mathbf{p}_i^2/\alpha) - 0.5 \sum_{i \neq j}^{N} \mathbf{p}_i \cdot \mathbf{T}_{ij} \cdot \mathbf{p}_j \\ &= -0.5 \sum_{i=1}^{N} \mathbf{p}_i \cdot \mathbf{E}_i^q ,\end{aligned} \tag{10}$$

therefore, from Eq. (10) and by recalling Eq. (1), we have that

$$\left(\frac{\partial U_{\mathrm{pol}}}{\partial \mathbf{p}_i} \right) = -\mathbf{E}_i^q - \sum_{i \neq j}^{N} (\mathbf{T}_{ij} \cdot \mathbf{p}_j - \mathbf{p}_i/\alpha) = 0, \tag{11}$$

i.e., the induced dipoles adjust themselves to minimize U_{pol}.[15] This also means that the contributions from induced dipoles do not depend on derivatives of dipole moments (they depend on explicit functions of distances).

Finally, the total potential energy for a system of N water molecules described by the self-consistent point dipole polarizability model (SCPDP) becomes

$$\begin{aligned}U_{\mathrm{SCPDP}} = 0.5 \sum_{i,j=1}^{N} \left[\sum_{\beta=1}^{3} \sum_{\gamma=1}^{3} \frac{q_i^\beta q_j^\gamma}{|\mathbf{r}_i^\beta - \mathbf{r}_j^\gamma|} - \mathbf{p}_i \cdot \mathbf{E}_i^q \right] \\ + 4\epsilon_{\mathrm{OO}} \sum_{i \neq j}^{N} \left[\left(\frac{\sigma_{\mathrm{OO}}}{|\mathbf{r}_i^4 - \mathbf{r}_j^4|} \right)^{12} - \left(\frac{\sigma_{\mathrm{OO}}}{|\mathbf{r}_i^4 - \mathbf{r}_j^4|} \right)^{6} \right],\end{aligned} \tag{12}$$

where the oxygen site is taken as the fourth site in the model's geometry, i.e., $\beta = \gamma = 4$ for the non-Coulombic O–O interactions.

B. Simulation methodology

The Newton–Euler equations of motion were integrated via Gear's fourth order predictor-corrector algorithm[30] with a Gaussian thermostat, as described in greater detail elsewhere.[31] All simulations were performed in the canonical-isokinetic (NVT) ensemble, with $N = 256$ particles at the system density and temperature of $\rho = 1.0$ g/cm^3 and $T = 298$ K, respectively. Standard periodic boundary conditions were used along with the minimum image criterion, a spherical center-to-center cutoff for the truncated intermolecular interactions, and a Verlet neighbor list. Long-ranged Coulombic interactions were corrected by a molecular reaction field with a dielectric constant $\epsilon_{\mathrm{rf}} = 78$[32] as described in the Appendix. Due to the efficient Gaussian thermostating, we found no need for a tapering of the truncated electrostatic potential to eliminate the eventual energy drift which usually appears in unthermostated simulations as a consequence of the truncation[33] and, according to Tildesley,[34] the use of periodic boundary conditions. The pressure and configurational internal energy were corrected by adding the usual long-range contributions assuming a uniform distribution beyond the cutoff distance r_c,[33] which in this case is $r_c \approx 9$ Å. With the resulting force fields we performed additional simulations at $T = 573$ K and 0.72 g/cc with $\epsilon_{\mathrm{rf}} = 20$.

The electrostatic charges for any geometry were chosen to match the permanent dipole moment of the isolated water molecule, 1.85 D.[28] Thus the resulting permanent quadrupoles are determined accordingly (see Table I). The electrostatic equation (1) with the experimental value for the molecular polarizability α=1.444 Å^3 [28] was solved to self-consistency every time step by a simple first order predictor-iterative method as suggested by Ahlström *et al.*,[15] during which the six elements of the dipole propagation tensor for each pair interactions were stored to avoid unnecessary recalculations. By initializing the induced dipoles with the self-consistent values of the previous time step, the method converged after two iterations at which the largest variation of any of the three component of the induced dipole was smaller than 0.005 D.

The first simulation started from an equilibrated configuration of the SPC model at the same state conditions. Subsequently, for each new geometry, the initial configuration was taken from an equilibrated one from a previous geometry. In order to determine the Lennard-Jones parameters for the model we targeted the configurational energy and pressure through a weak coupling to the force-field parameters ϵ_{OO} and σ_{OO}, to mimic the experimental values, respectively.[35] After a 10 ps equilibration, we perform a 40 ps simulation during which we obtained the time averages of the thermophysical and structural properties, including the corresponding force-field parameters. For the high temperature simulations, the initial configurations were taken from equilibrated ones at ambient conditions, after a simple coordinate and momentum scaling to satisfy the new density and temperature, respectively.

III. SIMULATION RESULTS AND DISCUSSION

As mentioned in Sec. I, our objective is the parameterization of a polarizable water model within a simple rigid geometry (Fig. 1) capable of reproducing the pressure and the configurational internal energy as well as the site–site pair correlation functions at 298 K and 1.0 g/cc. For all simulations at ambient conditions the configurational internal energy and pressure were obtained within $\pm$0.12 Kcal/mol and $\pm$0.04 Kbars from the experimental values of $-$9.92 Kcal/mol and 0.0 Kbars, respectively.

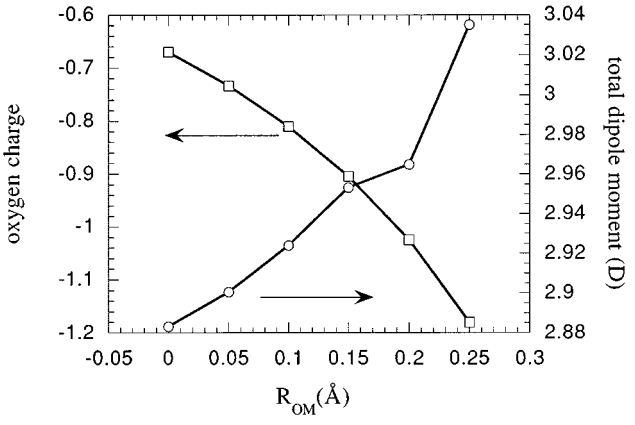

FIG. 3. Dependence of the total dipole moment and permanent negative charge with the distance R_{OM} for the water model at ambient conditions.

In Table II and Fig. 2 we display the resulting Lennard-Jones force-field parameters ϵ_{OO} and σ_{OO} corresponding to the desired geometries. In Fig. 3 we present the observed R_{OM} depedence for the negative charge and the total dipole moment, while in Figs. 4–6, the simulated site–site radial distribution functions for each geometry in comparison with the experimental results from neutron scattering.[36]

Our simulation results indicate that, in principle, it is possible to parameterize successfully the SCPDP model to represent accurately the pressure and configurational internal energy of water at ambient conditions, in a wide range of R_{OM}, i.e., $0 \leqslant R_{OM} \leqslant 0.25$ Å. The fact that the σ_{OO} (R_{OM}) and ϵ_{OO} (R_{OM}) exhibit a monotonic dependence with R_{OM} (Fig. 2) lends confidence to the parameterization methodology based on the weak coupling. Similar behavior is found for the induced (Table II) and total dipole moments (Fig. 3). Note, however, that the magnitude of the total dipole mo-

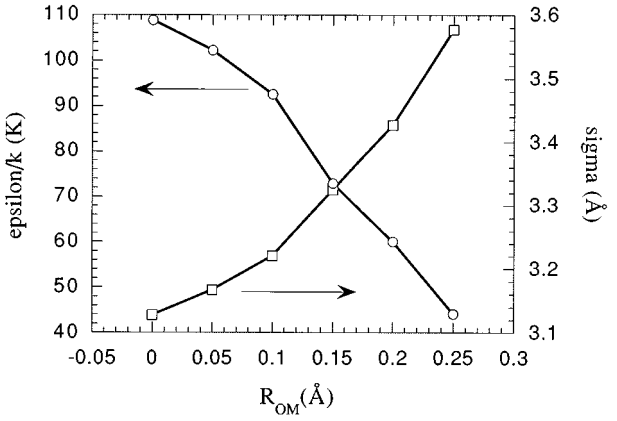

FIG. 2. Dependence of the Lennard-Jones force-field parameters ϵ_{OO} and σ_{OO} with the distance R_{OM} for the water model at ambient conditions. Uncertainties are indicated in Table II.

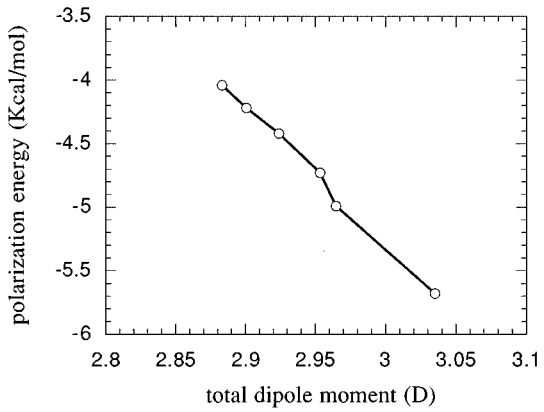

FIG. 4. Dependence of the polarization energy with the total dipole moment for the water model at ambient conditions.

TABLE II. Thermophysical properties and force-field parameters for the water models as a function of the adopted geometry.

R_{OM} (Å)	p (D)[a]	U_{pol} (kcal/mol)	epsilon/k (K)	sigma (Å)
0.0	1.05±0.03	−4.04±0.20	108.85±5.6	3.128±0.02
0.05	1.06±0.03	−4.22±0.15	102.18±1.3	3.167±0.01
0.10	1.10±0.03	−4.42±0.15	92.56±2.6	3.221±0.01
0.15	1.11±0.03	−4.93±0.23	72.92±1.0	3.325±0.01
0.20	1.14±0.03	−4.99±0.14	60.00±0.6	3.427±0.06
0.25	1.21±0.03	−5.68±0.23	44.17±1.6	3.577±0.01

[a]Note that $|m|=(1.85+|p|\langle\cos\theta\rangle)$D (see the text).

ment is $|m|=(1.85+|p|\langle\cos\theta\rangle)$D, where θ is the angle between the permament and the induced dipoles. For the chosen geometries, $0.93<\langle\cos\theta\rangle<0.95$, i.e., $18^0<\theta<22^0$ for $0\geqslant R_{OM}\geqslant 0.25$ Å.

Not surprisingly, the total dipole moment increases with the increasing oxygen charge, since a greater charge induces a larger polarization at constant permanent dipole moment (see Figs. 3 and 4). If we assume that the total (permanent plus induced) dipole moment of water at ambient conditions is (according to the calculated value for ice,[28,37] theoretical results,[3] and *ab initio* simulations[38]) in the range of 2.40–3.27 D, all geometries of the proposed polarizable model predict a polarization within the above interval, though larger than the most frequently quoted value of 2.6 D which corresponds to ice rather than ambient water.[39]

The observed polarization behavior is clearly the consequence of assuming simple point (rather than distributed) charges for the O–O Coulombic interactions, a feature that might induce a polarization catastrophe if the repulsive part of the Lennard-Jones allowed encounters closer than $\sqrt[6]{4\alpha^2}$, i.e., 1.42 Å for $\alpha=1.444$ Å^3.[15] Furthermore, the observed high polarization, which accounts for 40%–57% of the total configurational internal energy (Table II), translates into stronger O–O and O–H interactions as R_{OM} becomes larger, as clearly seen in the site–site radial distribution functions presented in Figs. 5–7.

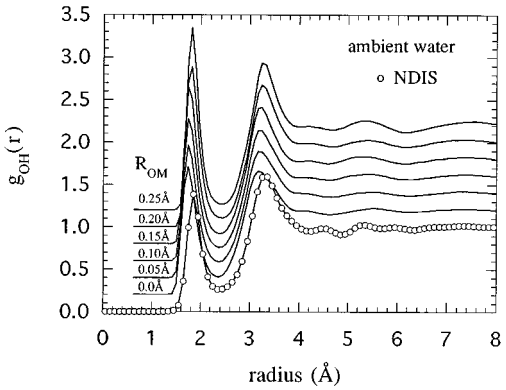

FIG. 6. Comparison between the experimental NDIS and the simulated O–H radial distribution functions of ambient water for five R_{OM} values, each shifted by 0.2 unity for clarity. Symbols indicate NDIS results of Soper and Phillips (Ref. 36).

Yet, the proposed model (with its five different values of R_{OM}) captures the main features of the experimental site–site radial distribution functions, although the agreement with experiment is not as good as those for the SPC[6] and TIP4P[8] nonpolarizable models; they show defects specific to the way we introduce polarization. For example, the simulated $g_{OO}(r)$ for $R_{OM}=0$ shows little structure after the first peak, a common problem already seen by others[15,26] for a similar geometry but different force fields, and a clear skewness in the second peak of $g_{OO}(r)$ for $0\leqslant R_{OM}\leqslant 0.1$ Å. Thus the lack of a well-defined and properly located second peak in the $g_{OO}(r)$, i.e., around $r=4.5$ Å, indicates that for this geometry the model is not able to describe fully the tetrahedral water structure.[36] While an increase of R_{OM} beyond 0.1 Å induces a better structure for the second peak of the $g_{OO}(r)$, it also results in an overestructured first peak. A similar situation is observed in the behavior of $g_{OH}(r)$, where an increase of R_{OM} shifts the first and second peaks right toward their proper location at the expense of an overcorrelation for the first peak (see Fig. 6). The impact of R_{OM} on the $g_{HH}(r)$ is

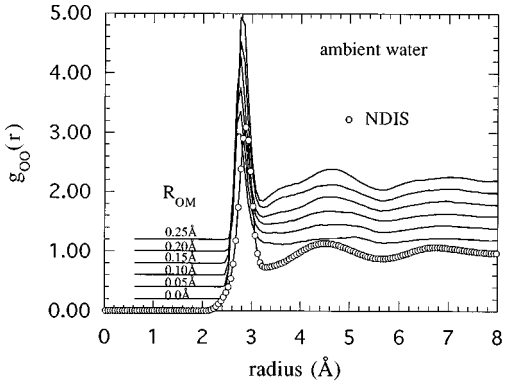

FIG. 5. Comparison between the experimental NDIS and the simulated O–O radial distribution functions of ambient water for five R_{OM} values, each shifted by 0.2 unity for clarity. Symbols indicate NDIS results of Soper and Phillips (Ref. 36).

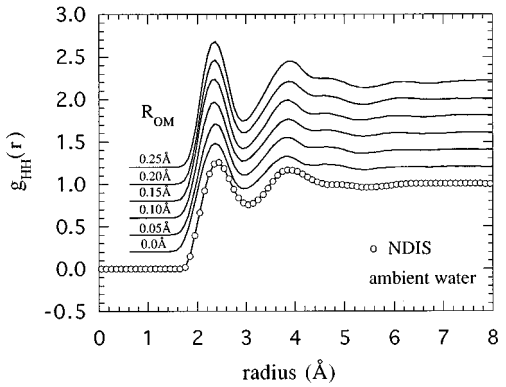

FIG. 7. Comparison between the experimental NDIS and the simulated H–H radial distribution functions of ambient water for five R_{OM} values, each shifted by 0.2 unity for clarity. Symbols indicate NDIS results of Soper and Phillips (Ref. 36).

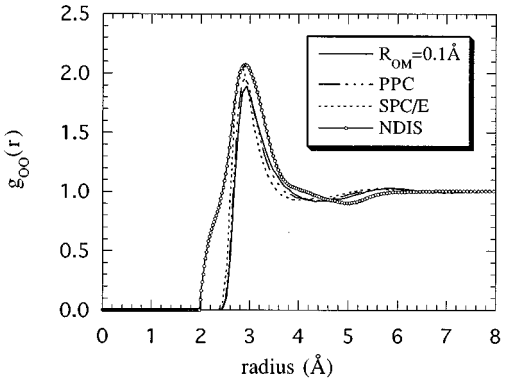

FIG. 8. Comparison between the experimental NDIS and the simulated O–O radial distribution functions of water at 573 K and 0.72 g/cc. Symbols indicate NDIS results of Postorino *et al.* (Ref. 27).

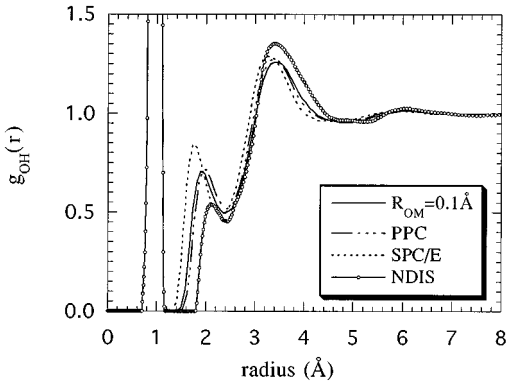

FIG. 9. Comparison between the experimental NDIS and the simulated O–H radial distribution functions of water at 573 K and 0.72 g/cc. Symbols indicate NDIS results of Postorino *et al.* (Ref. 27).

less pronounced than that for the other site–site correlation functions, though the trend is the same as for $g_{OO}(r)$ and $g_{OH}(r)$, i.e., the larger the R_{OM} the stronger the correlation.

The described features, in addition to the fact that the proposed model shows an approximately correct quadrupole moment for $R_{OM} \approx 0.2$ Å (see Table I), lend support to the contention that, regardless of the adopted geometry and the magnitude of the charges, a successful model should describe not only the correct permanent dipole but also the accurate effective quadrupole moment. In fact, Carnie and Patey[3] showed that the quadrupole moment of waterlike molecules has a strong effect on the fluid's structure, and consequently on the dielectric behavior through Kirkwood's G_k factor,[40] by effectively quenching the strong dipole–dipole correlations.

The absence of polarization damping at short range can be expected to lead to stronger pair correlations, and according to earlier studies,[3,41,42] to unrealistic large dielectric constants. The structural results in Figs. 5–7, in conjunction with the charge and polarization data of Tables I and II, are consistent with the idea that our polarizable model, based on point charges, suffers from an absence of polarization damping at short range. Even so, the model provides a convenient reference model to analyze and understand how the polarization behaves in a more compressible region of the phase diagram, and its microstructural implications. With that purpose we use the parameterized model with R_{OM}=0.1 Å, a geometry that exhibits reasonable polarizable and microstructural behavior in comparison with the available experimental data. The results of this study are presented in Figs. 8–10 where we display the high temperature site-site microstructure of the proposed polarizable model in comparison to that of the nonpolarizable SPC/E model, the polarizable point charge (PPC) model,[24] and the NDIS experiments.

In order to make some sense of this structural comparison we must invoke Löffler *et al.*'s compelling analysis[43] of Postorino *et al.*'s NDIS results[27] (see the final discussion regarding Figs. 3 and 4 of Ref. 43). Löffler *et al.* provided evidence to support the claim of a common source for the observed weakening of the first peak of the $g_{OH}(r)$ and the unphysical correlation enhancement at the base of the first peak of the $g_{OO}(r)$. According to our simulation results, Figs. 8–10, the proposed polarizable model gives a first peak shifted 0.2 Å to the right and weaker than that for the for the $g_{OH}(r)$ of the SPC/E and other models.[12] Note that according to Löffler *et al.*'s analysis, neither the location of the first peak nor the size and shape of the second peak of the $g_{OH}(r)$ is affected by the problem they pinpointed in the processing of the experimental data. Consequently, the comparison in Fig. 9 suggests that, even though the present polarizable model overestimates the polarization (short-range behavior), it also gives an overall better representation for the $g_{OH}(r)$ than the common nonpolarizable models at high temperature over the range of r in which the NDIS results can be relied upon. By the same token, Fig. 10 suggests that our model gives a remarkably good description of the $g_{HH}(r)$. However, little can be said about the $g_{OO}(r)$ since this is the least accurately determined by the neutron scattering experiments (Fig. 8).[43] Our model exhibits a qualitative agreement with the NDIS, beyond the problem with the shoulder on the left side of the first peak of the $g_{OO}(r)$, whose meaning has been already discussed by Löffler *et al.*[43]

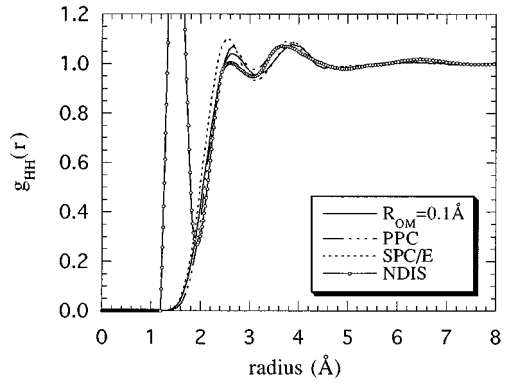

FIG. 10. Comparison between the experimental NDIS and the simulated H–H radial distribution functions of water at 573 K and 0.72 g/cc. Symbols indicate NDIS results of Postorino *et al.* (Ref. 27).

With regards to the thermophysical properties, the total dipole moment decreases from 2.92 ± 0.02 to 2.4 ± 0.1 D (in a remarkable good agreement with the *ab initio* simulation result of 2.3 ± 0.2 D[44]), with a polarization energy decreasing from -4.42 ± 0.2 to -1.59 ± 0.1 Kcal/mol. This total dipole moment compares very well with the effective (permanent) dipole moment of the SPC/E model, i.e., 2.35 D, while the predicted structure appears to be in better agreement with the NDIS results (specially the position of the first peak of $g_{\mathrm{OH}}(r)$ than that of the SPC/E model. Interestingly, the PPC model with a permanent dipole moment of 2.14 D predicts not only a structure very similar to that of the proposed model (see Figs. 8–10), but also a total dipole moment of 2.38 ± 0.05 D.[45]

In summary, the parameterized model is able to describe accurately the pressure and configurational energy of water at ambient conditions, while having the experimental value for the permanent dipole moment. The resulting structure shows evidence of overstructuring induced by the short-range dipole overpolarization, a clear manifestation of the unrealistic Coulombic description through point charges. The reported results highlight the shortcomings of this approximation for the polarization behavior at short intermolecular distances, and provide a meaningful starting point from which we can attempt to overcome the mentioned defects. Work in this direction is already in progress.

ACKNOWLEDGMENTS

This work was supported by the Division of Chemical Sciences, Office of Basic Energy Sciences, U.S. Department of Energy. Some of the computations reported in this work were performed on IBM RS/6000 in the Computational Laboratory for Environmental Biotechnology in the Department of Chemical Engineering at the University of Virginia. The authors also acknowledge fruitful discussions with Igor Svishchev and Peter G. Kusalik.

APPENDIX: REACTION FIELD EXPRESSIONS FOR THE TOTAL ELECTRIC FIELD AND ELECTROSTATIC ENERGY

If the electrostatic interactions are truncated at a center of mass distance r_c, and the long range contributions accounted for a reaction field, Eq. (2) becomes[32]

$$\mathbf{E}_i^q=\left[\sum_{j\neq i,\gamma}^{N} q_j^{\gamma}\frac{\mathbf{r}_{i,j\gamma}}{r_{i,j\gamma}^3}\right]_{r_{ij}<r_c}+\mathrm{RF}\sum_{j}^{N}\boldsymbol{\mu}_j$$

$$=\left[\sum_{j\neq i,\gamma}^{N} q_j^{\gamma}\mathbf{r}_{i,j\gamma}\left(\frac{1}{r_{i,j\gamma}^e}-\mathrm{RF}\right)\right]_{r_{ij}<r_c}+\mathrm{RF}\boldsymbol{\mu}_i \tag{A1}$$

while Eq. (3) becomes

$$\mathbf{E}_i^p=\left[\sum_{j\neq i}^{N}(\mathbf{T}_{ij}+\mathrm{RF}I)\cdot\mathbf{p}_j\right]_{r_{ij}<r_c}+\mathbf{RF}\mathbf{p}_i\,, \tag{A2}$$

where $\boldsymbol{\mu}_i$ is the permanent dipole moment of molecule i, $\boldsymbol{\mu}_i=\Sigma_\beta q_i^\beta\mathbf{r}_i^\beta$, with

$$\mathrm{RF}=\frac{2(\epsilon_{\mathrm{rf}}-1)}{(2\epsilon_{\mathrm{rf}}+1)r_c^3} \tag{A3}$$

and ϵ_{rf} being the dielectric constant of the reaction field. Consequently, Eq. (6) reduces to

$$U_{qq}=0.5\left[\sum_{j\neq i}^{N}\sum_{\beta,\gamma}^{s}\frac{q_i^\beta q_j^\gamma}{r_{i\beta,j\gamma}}\right]_{r_{ij}<r_c}-0.5\ \mathrm{RF}\sum_{i,j}^{N}\boldsymbol{\mu}_i\cdot\boldsymbol{\mu}_j\,. \tag{A4}$$

Now, by recalling the electroneutrality condition $\Sigma_\beta q_i^\beta=0$, the dipole scalar product $\boldsymbol{\mu}_i\cdot\boldsymbol{\mu}_j$ can also be written as

$$\boldsymbol{\mu}_i\cdot\boldsymbol{\mu}_j=\sum_{\beta,\gamma}^{s}q_i^\beta q_j^\gamma(\mathbf{r}_i^\beta\cdot\mathbf{r}_j^\gamma)$$

$$=0.5\sum_{\beta,\gamma}^{s}q_i^\beta q_j^\gamma(r_i^{\beta2}-r_j^{\gamma2}-(r_i^\beta-r_j^\gamma)^2)$$

$$=-0.5\sum_{\beta,\gamma}^{s}q_i^\beta q_j^\gamma(r_i^\beta-r_j^\gamma)^2 \tag{A5}$$

after invoking the square of the vector $\mathbf{r}_{i\beta,j\gamma}=\mathbf{r}_i^\beta-\mathbf{r}_j^\gamma$. Finally,

$$U_{qq}=0.5\left[\sum_{j\neq i}^{N}\sum_{\beta,\gamma}^{s}\frac{q_i^\beta q_j^\gamma}{r_{i\beta,j\gamma}}\right]_{r_{ij}<r_c}$$

$$+0.25\ \mathrm{RF}\left[\sum_{j\neq i}^{N}\sum_{\beta,\gamma}^{s}q_i^\beta q_j^\gamma r_{i\beta,j\gamma}^2-\frac{\mu^2}{r_c^3}\right], \tag{A6}$$

where $\mu\equiv|\boldsymbol{\mu}_i|$.

[1] D. L. Beveridge, M. Mezei, P. K. Mehrotra, F. T. Marchese, G. Ravi-Shanker, T. Vasu, and S. Swaminathan, in *Molecular-Based Study of Fluids*, edited by J. M. Haile and G. A. Mansoori, ACS Advances in Chemistry Series No. 204 (American Chemical Society, Washington, D.C., 1983).
[2] F. H. Stillinger, Science **209**, 451 (1980).
[3] S. L. Carnie and G. N. Patey, Mol. Phys. **47**, 1129 (1982).
[4] C. D. Berweger, W. F. van Gunsteren, and F. Müller-Plathe, Chem. Phys. Lett. **232**, 429 (1995).
[5] A. A. Chialvo, J. Chem. Phys. **104**, 5240 (1996).
[6] H. J. C. Berendsen, J. P. M. Postma, W. F. van Gunsteren, and J. Hermans, in *Intermolecular Forces: Proceedings of the Fourteenth Jerusalem Symposium on Quantum Chemistry and Biochemistry*, edited by B. Pullman (Reidel, Dordrecht, 1981), pp. 331–342.
[7] H. J. C. Berendsen, J. R. Grigera, and T. P. Straatsma, J. Phys. Chem. **91**, 6269 (1987).
[8] W. L. Jorgensen, J. Chandrasekhar, J. D. Madura, R. W. Impey, and M. L. Klein, J. Chem. Phys. **79**, 926 (1983).
[9] F. H. Stillinger and A. Rahman, J. Chem. Phys. **60**, 1545 (1974).
[10] J. J. de Pablo, J. M. Prausnitz, H. J. Strauch, and P. T. Cummings, J. Chem. Phys. **93**, 7355 (1991).
[11] Y. Guissani, and B. J. Guillot, J. Chem. Phys. **98**, 8221 (1993).
[12] A. A. Chialvo and P. T. Cummings, J. Phys. Chem. **100**, 1309 (1996).
[13] J. A. C. Rullmann and P. T. van Duijnen, Mol. Phys. **63**, 451 (1988).
[14] M. Sprik and M. L. Klein, J. Chem. Phys. **89**, 7556 (1988).
[15] P. Ahlström, A. Wallqvist, S. Engström, and B. Jönsson, Mol. Phys. **68**, 563 (1989).
[16] S. Kuwajima and A. Warshel, J. Phys. Chem. **94**, 460 (1990).
[17] S.-B. Zhu, S. Singh, and G. W. Robinson, J. Chem. Phys. **95**, 2791 (1991).
[18] L. X. Dang, J. Chem. Phys. **97**, 2659 (1992).
[19] E. Clementi, G. Corongiu, and F. Sciortino, J. Mol. Struc. **296**, 205 (1993).

[20] G. Corongiu and E. Clementi, J. Chem. Phys. **98**, 4984 (1993).
[21] S. W. Rick, S. J. Stuart, and B. J. Berne, J. Chem. Phys. **101**, 6141 (1994).
[22] J. Brodholt, M. Sampoli, and R. Vallauri, Mol. Phys. **86**, 149 (1995).
[23] J. Brodholt, M. Sampoli, and R. Vallauri, Mol. Phys. **85**, 81 (1995).
[24] P. T. Kusalik and I. M. Svishchev, Science **265**, 1219 (1994).
[25] U. Niesar, G. Corongiu, E. Clementi, G. R. Kneller, and D. K. Bhattacharya, J. Phys. Chem. **94**, 7949 (1990).
[26] D. van Belle, M. Froyen, G. Lippens, and S. J. Wodak, Mol. Phys. **77**, 239 (1992).
[27] P. Postorino, R. H. Tromp, M. A. Ricci, A. K. Soper, and G. W. Neilson, Lett. Nature **366**, 668 (1993).
[28] D. Eisenberg and W. Kauzmann, *The Structure and Properties of Water* (Oxford University Press, New York, 1969).
[29] C. J. F. Böttcher, *Theory of Electric Polarization* (Elsevier, Amsterdam, 1973), Vol. 1.
[30] C. W. Gear, *The Numerical Integration of Ordinary Differential Equations of Various Orders* (Argonne National Laboratory, 1966).
[31] P. T. Cummings, A. A. Chialvo, and H. D. Cochran, Chem. Eng. Sci. **49**, 2735 (1994).
[32] O. Steinhauser, Mol. Phys. **45**, 335 (1982).
[33] M. P. Allen and D. J. Tildesley, *Computer Simulation of Liquids* (Oxford University Press, Oxford, 1987).
[34] D. J. Tildesley, in *Molecular Liquids. Dynamics and Interactions*, edited by A. J. Barnes (Reidel, Dordrecht, 1984); Vol. C135, pp. 519–560. See Fig. 4(a) and preceding text.
[35] S. L. Njo, W. F. van Gunsteren, and F. Müller-Plathe, J. Chem. Phys. **102**, 6199 (1995).
[36] A. K. Soper and M. G. Phillips, Chem. Phys. **107**, 47 (1986).
[37] E. Whalley, J. Glaciology **21**, 13 (1978).
[38] K. Laasonen, M. Sprik, M. Parrinello, and R. Car, J. Chem. Phys. **99**, (1993).
[39] C. A. Coulson and D. Eisenberg, Proc. R. Soc. London A **291**, 445 (1966).
[40] M. Neumann, Mol. Phys. **50**, 841 (1983).
[41] K. Watanebe and M. L. Klein, Chem. Phys. **131**, 157 (1989).
[42] M. Sprik, J. Chem. Phys. **95**, 6762 (1991).
[43] G. Löffler, H. Schreiber, and O. Steinhauser, Ber. Bunsenges. Phys. Chem. **98**, 1575 (1994).
[44] E. S. Fois, M. Sprik, and M. Parrinello, Chem. Phys. Lett. **223**, 411 (1994).
[45] A. A. Chialvo and P. T. Cummings, in *Annual AICHE Meeting*, Miami Beach (1995).
[46] J. Verhoeven and A. Dymanus, J. Chem. Phys. **52**, 3222 (1970).